Chapter 7

Application of 2D Materials to Ultrashort Laser Pulse Generation

Grzegorz Sobon

Additional information is available at the end of the chapter

http://dx.doi.org/10.5772/63336

Abstract

In recent years, novel two-dimensional (2D) materials have revolutionized the field of ultrafast laser technology. They have emerged as efficient, cost-effective, and universal saturable absorbers for the so-called ultrafast lasers, which emit ultrashort optical pulses (on the timescale of femtoseconds). Thanks to their unique optical properties, such as broadband absorption, short recovery time, low saturation fluence, and high modulation depth, they might be used as saturable absorbers for different lasers (solid state, fiber, semiconductor) operating at different wavelengths (ranging from 500 to 2500 nm). Such lasers may find various applications in different areas of industry, medical procedures, precise metrology, gas sensing, laser spectroscopy, etc. This chapter discusses the recent achievements in the area of ultrafast fiber lasers utilizing 2D materials: graphene, topological insulators (Bi_2Te_3, Bi_2Se_3, Sb_2Te_3), transition metal dichalcogenides (MoS_2, WS_2, etc.), and black phosphorus. The optical properties of those materials will be described. Their usability in ultrafast photonics will be discussed.

Keywords: 2D materials, mode-locked lasers, ultrafast lasers, graphene, saturable absorbers

1. Introduction

Atomically thin layered materials, usually referred to as 2D materials or low-dimensional materials, are often characterized by unique and unexpected electronic and optical properties. The most popular example of a 2D material is graphene, which is composed of a single layer of carbon atoms, forming a 2D honeycomb lattice. Graphene is a fundamental building block of three-dimensional (3D) graphite. The growing interest in novel two-dimensional materials started in 2004 after the discovery of unique electrical properties of graphene [1]. After that

success, the scientists around the world extensively investigate other thin layered materials, such as topological insulators (TIs), transition metal dichalcogenides (TMDCs), black phosphorus (BP), and many others.

The popularity of 2D materials among researchers is mainly driven by their unique electrical properties and their potential applications in new-generation electronic devices. However, those materials are also characterized by multiple unique optical properties, such as broadband and almost wavelength-independent absorption or optical bistability (saturable absorption with ultrashort recovery time and high modulation depth). Those properties make 2D materials useful in laser technology, e.g., as saturable absorbers for lasers emitting ultrashort optical pulses. The so-called mode-locked lasers, emitting ultrashort pulses in the infrared range, are currently on demand of many industrial, military, and medical applications. They might be used in many various fields, e.g., in medicine and surgery [2], materials processing [3], laser spectroscopy [4, 5], and fundamental science (generation of terahertz waves [6], multiphoton systems for optical imaging [7], or supercontinuum generation [8]). Ultrafast lasers are also main building blocks of optical frequency combs, which are currently used in, e.g., spectrograph calibration enabling detection of extrasolar planets [9] or optical-atomic clocks [10]. The research on novel 2D materials strongly contributes to the development of novel laser sources, enabling generation of shorter pulses and broader bandwidths at new wavelength regions, previously uncovered by any other coherent light source. This chapter explains the fundamentals of ultrashort pulse generation and reviews and summarizes the most important recent achievements in the field of ultrafast lasers incorporating 2D materials.

2. Saturable absorbers

2.1. Saturable absorption effect

Saturable absorption (SA) is a nonparametric nonlinear optical process, which occurs in many materials under excitation with high-power light beam. In general, the optical transmittance of a saturable absorber is power dependent in a way that it introduces larger losses for low-intensity light. After illumination with high-intensity light, the absorption saturates and the SA becomes more transparent. A saturable absorber is characterized by three main parameters: its modulation depth (α_0), saturation intensity or saturation fluence (I_{sat}/F_{sat}), and nonsaturable losses (α_{NS}). All those parameters are bound with a simple formula, which describes the power-dependent absorption $\alpha(I)$ of a two-level saturable absorber [11]:

$$\alpha(I) = \frac{\alpha_0}{1 + \frac{I}{I_{sat}}} + \alpha_{NS} \tag{1}$$

http://dx.doi.org/10.5772/63336

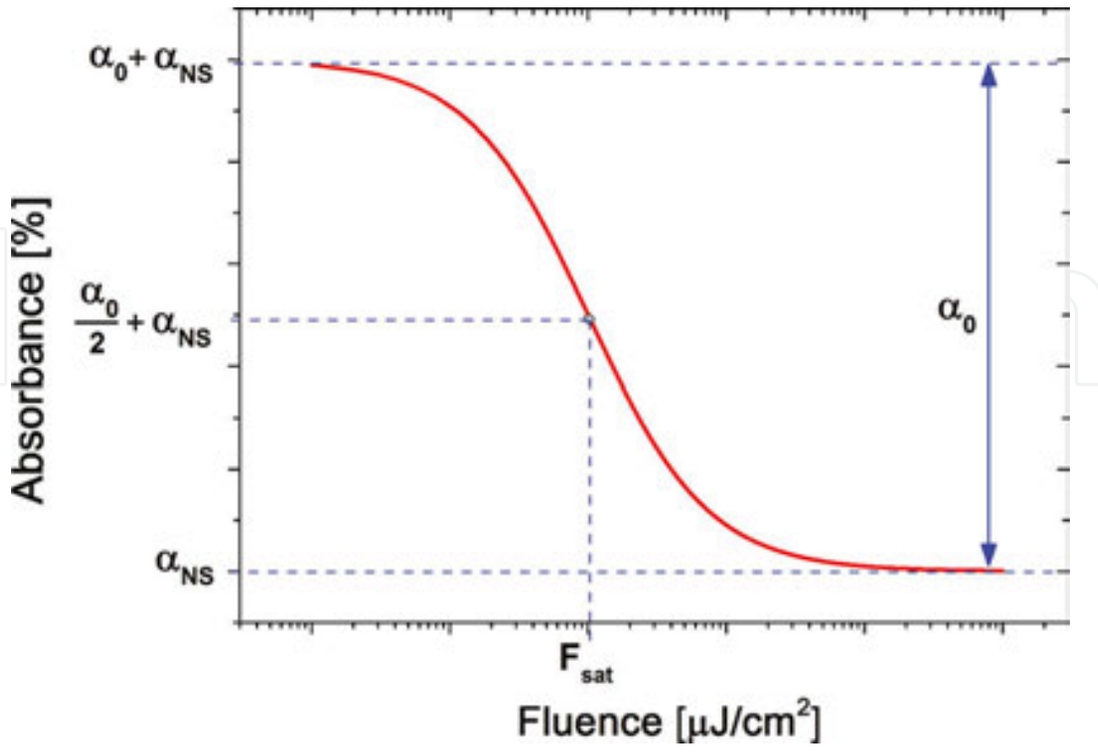

Figure 1. Theoretical saturable absorption curve calculated from formula (1) with indicated three main parameters of a saturable absorber.

The modulation depth can be understood as the contrast ratio between the "on" and "off" states of the SA, i.e., the difference between the minimum and maximum transmission. The nonsaturable loss is a constant linear loss level, which cannot be saturated. The saturation fluence (or saturation intensity) is usually defined as the incident fluence (or intensity) needed to achieve half of the modulation depth. A typical saturable absorption curve calculated with the use of formula (1) is plotted in **Figure 1** together with indicated parameters (note that the *X*-axis is in the logarithmic scale). Alternatively, the *Y*-axis might be scaled in the transmittance value.

2.2. Mode locking of lasers using saturable absorbers

Thanks to its "bistable" nature, a saturable absorber might act as a very fast optical switch when inserted into a laser cavity. A simplified schematic of a laser resonator incorporating a saturable absorber is depicted in **Figure 2(a)**. After turning on the laser (i.e., pumping the gain medium), the saturable absorber is in its "off" state, introducing quite high losses, which predominate the laser gain (see **Figure 2(b)**). After a short period of time (e.g., few hundreds of cavity roundtrips), an optical pulse will spontaneously arise from the continuous wave (CW) noise. If the intensity of the pulse will be high enough, it will pass through the SA with smaller losses than the CW noise. In consequence, a short pulse might be emitted from such laser [12]. An ultrashort pulse is always an effect of constructive interference between a certain number of longitudinal modes in the cavity. In order to achieve this interference, the consequent modes need to have fixed phase relationship with each other. In other words, the phase of the modes

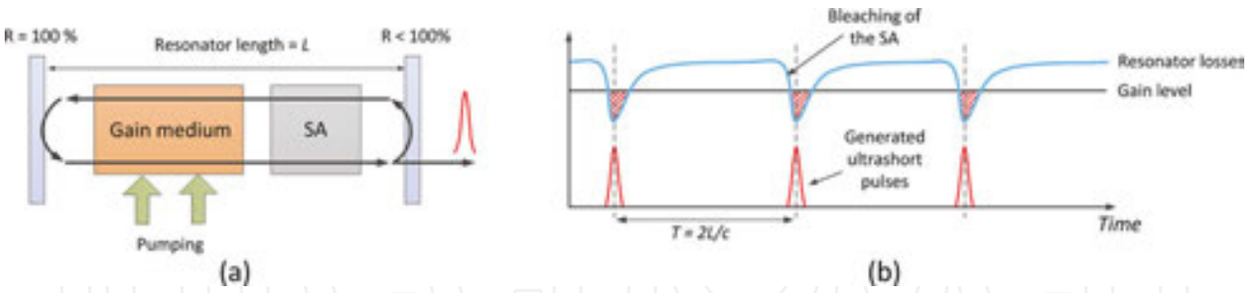

Figure 2. Illustration of a laser cavity with inserted saturable absorber (a) and pulse train formed in the cavity as a result of resonator loss modulation (b).

needs to be locked ("mode locking"). If the modes would oscillate randomly (without phase coherence), the output radiation would be multimode, continuous wave (CW). When the phases of the modes are locked, the laser will generate optical pulses according to the rule: more synchronized modes—shorter pulses.

There are several types of saturable absorbers currently used in laser technology. They can be generally classified into two categories: artificial and real SAs (see **Figure 3**). The term "artificial SA" refers to a mode-locking technique, where a nonlinear optical effect (which is power dependent) acts as a saturable absorber. Among those techniques, the most important include nonlinear polarization rotation (NPR), nonlinear loop mirrors (NOLM) or nonlinear amplifying loop mirror (NALM), and Kerr-lens mode locking (KLM).

Among real saturable absorbers we can distinguish two groups: semiconductors (so-called semiconductor saturable absorber mirrors, SESAMs) and nanomaterials. The SESAMs are currently one of the most widely used saturable absorbers in solid-state and fiber lasers, also in commercially available industrial systems. They are based on a well-established technology developed for more than 20 years [13]. However, SESAMs have some limitations. The technology is based on semiconductors (e.g., InGaAs/GaAs quantum wells), which are characterized by an energy band gap. Consequently, this results in a limited wavelength operation range. Thus, each SESAM needs to be designed strictly for a specific laser (operating at a certain wavelength). Fabrication of the SESAM also involves expensive and complicated molecular beam epitaxy (MBE) technology [14]. All those limitations have driven the laser community to seek for alternative, new saturable absorber materials. The field of nanomaterial-based SAs emerged in recent years to one of the most important branches of ultrafast laser technology. This new era started in 2003 as Set et al. [15] demonstrated the first CNT mode-locked fiber laser. Few years later, in 2009, the first lasers utilizing graphene were reported [16, 17]. Starting from this date, the number of papers and reports on fiber lasers mode-locked with graphene and other 2D materials: topological insulators, transition metal dichalcogenides, and recently black phosphorus, grow rapidly.

http://dx.doi.org/10.5772/63336

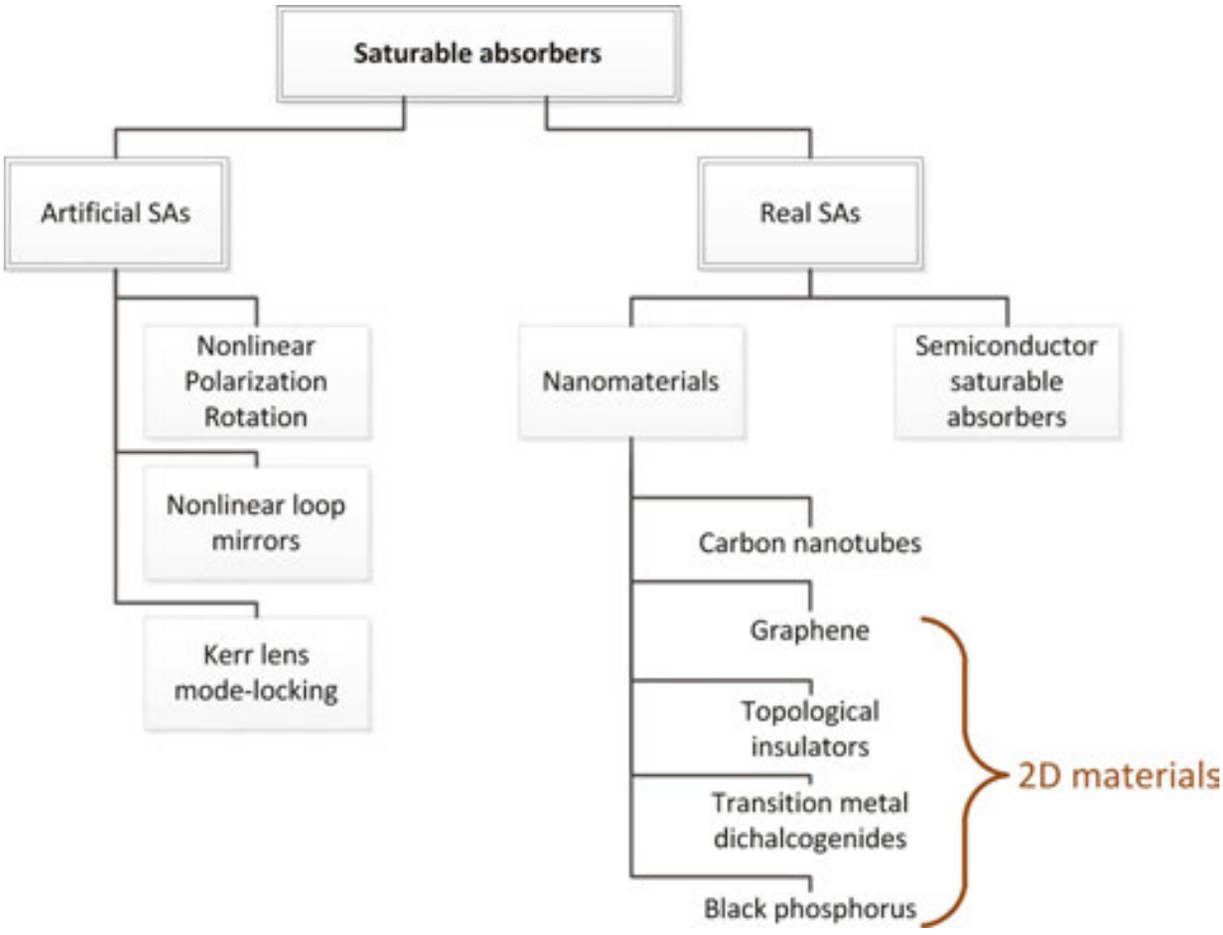

Figure 3. Types of saturable absorbers for ultrafast lasers.

There are several techniques of fabricating saturable absorber devices using 2D materials and make them suitable for use in a mode-locked laser, which might be either a solid-state or a fiber-based laser. The most popular approaches are illustrated in **Figure 4**.

The material might be deposited on a glass plate (plano window or a wedge) and inserted into the cavity as a free-space transmission saturable absorber (**Figure 4a**). This approach is most suitable for solid-state lasers [18–20]. For example, in the work of Ugolotti et al., a graphene monolayer grown via chemical vapor deposition (CVD) was transferred from a copper substrate on to a 1 mm thick quartz plate, with the use of poly(methylmethacrylate) (PMMA) polymer. Such SA exhibited 0.75% of modulation depth at 1 μm wavelength and supported mode locking with around 32 μm spot size on the graphene surface. Glass windows with deposited SA material might also be used in fiber lasers (e.g., with graphene [21]), but this approach seems not to be as efficient as the other methods. The world's first TI-based fiber laser used a Bi_2Te_3 layer deposited on a quartz plate and inserted into the cavity between two collimators [22].

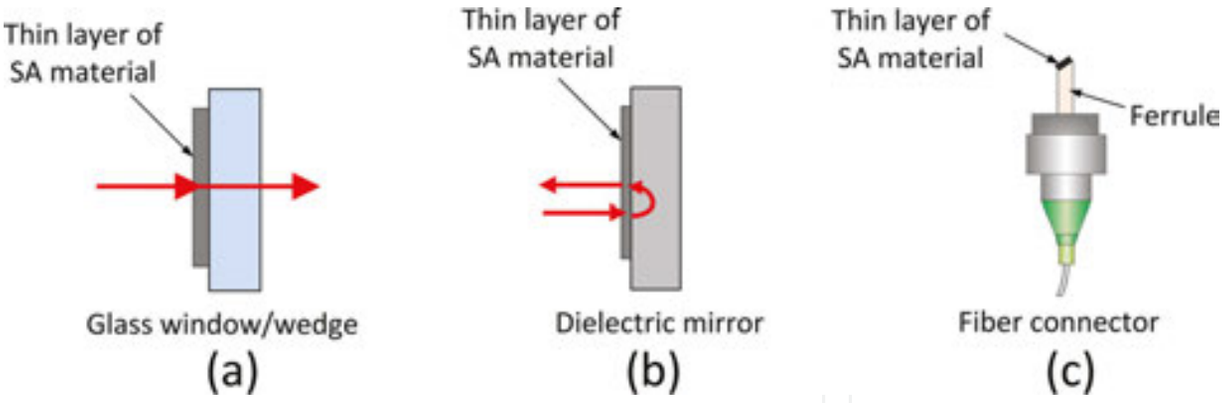

Figure 4. Common techniques of depositing SA material on optical substrates: on glass plates (a), mirrors (b), and fiber connectors (c).

The SA material might also be deposited on a mirror (**Figure 4b**) and inserted into a linear laser cavity (both fiber based or free space). In the case of a fiber ring-shaped resonator, one can use a circulator to couple the mirror with the cavity. This approach was used, e.g., by Xu et al. [23, 24] for the generation of femtosecond pulses from Er-doped fiber lasers. Graphene-coated mirrors might also serve as saturable absorbers in linear laser cavities as demonstrated by Cunning et al. [25]. However, usually graphene-coated mirrors serve as saturable absorbers for solid-state lasers [26–29]. The most impressive results were obtained by Ma et al. [29]. The SA was based on high-quality, CVD-grown monolayer graphene transferred onto a highly reflecting dielectric mirror. The spot size on the SA was about 60 μm. The laser was capable of generating 30 fs pulses at 50 nm bandwidth centered at 1070 nm [29].

The probably most popular and common technique of fabricating saturable absorbers with 2D materials is based on fiber connectors (as shown in **Figure 4c**). This approach was already demonstrated with graphene [30, 31], TIs [32, 33], TMDCs [34, 35], and BP [36, 37]. It is a very convenient method since it is alignment free and very robust. It allows to keep the cavity fully fiberized, which is very advantageous—the lasers are more compact, stable, and invulnerable to external disturbances.

The newest technique of SA fabrication is based on the evanescent field interaction effect. For this purpose, tapered fibers (microfibers) or side-polished (D-shaped) fibers might be used (**Figure 5**). The saturable absorption is based on the interaction between the evanescent field propagating in the cladding of the fiber and the deposited material. Such saturable absorbers were first used in combination with carbon nanotubes [38]. In 2010, Song et al. [39] demonstrated the usage of a graphene-coated D-shaped fiber as a saturable absorber. The laser was capable of generating pulses at 1561 nm with 2 nm of full width at half maximum (FWHM) bandwidth. Afterward, the deposition of TIs and TMDCs on such fibers was demonstrated [40, 41]. The alternative approach, using tapered fibers, is also commonly used and was demonstrated by several authors [42–46].

http://dx.doi.org/10.5772/63336

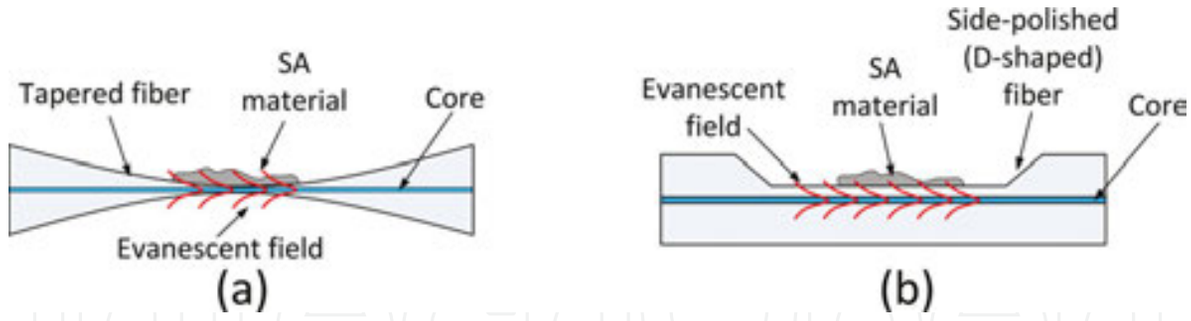

Figure 5. Saturable absorbers with evanescent field interaction: a fiber taper (a) and side-polished (D-shaped) fiber (b).

The performance of fiber lasers with evanescent field interaction is indisputable: 70 fs pulses were generated with a TI deposited on a tapered fiber [47], whereas Sb_2Te_2 deposited on a side-polished fiber allowed to achieve 128 fs pulses [48]. However, both techniques have some serious drawbacks. A saturable absorber based on a D-shaped fiber, due to its asymmetry, is always characterized by a polarization-dependent loss (PDL), which mostly depends on the material type (its refractive index), interaction length, and the distance between the polished region and the fiber core. In some reports, the PDL was kept at quite low levels (e.g., 1 dB in [49] with 6 μm distance between the material and the core), but sometimes it exceeds several dB [50]. In this situation, it is difficult to distinguish whether the mode locking originates from nonlinear polarization rotation or from the saturable absorption in the 2D material. In 2015, Bogusławski et al. [51] performed an experiment, which has unambiguously proven that mode locking in such oscillators is a combination of both effects. The study revealed that the hybrid mode-locking mechanism (combined NPR with saturable absorption of Sb_2Te_3 topological insulator) allows to achieve the best performance (in terms of bandwidth and pulse duration), when compared with a truly NPR or a TI-SA mode-locked laser. In the case of taper-based SAs, it is worth mentioning that in order to achieve sufficient interaction the fiber diameter needs to be reduced to less than 7 μm [42–45], which makes the taper quite long (from 5 to 18 cm waist length [44, 52]), and obviously much more fragile than a normal optical fiber. On the other hand, many authors who investigated evanescent field interaction claim higher optical power-induced damage threshold for such SA in comparison to connector end-face deposition due to better thermal management [39].

2.3. Nonlinear absorption measurements

The three basic nonlinear parameters of a saturable absorber (modulation depth, saturation fluence, and nonsaturable loss) might be measured in the so-called power-dependent transmission setup, which is depicted in **Figure 6**.

As a pumping source, an amplified pulsed laser (e.g., femtosecond or picosecond) is used in order to provide intensity high enough to saturate the saturable absorber. The beam from the laser is divided into two parts. The first beam acts as a reference channel and is directed to the power meter, whereas the second beam is focused by a lens and directed to the saturable absorber (e.g., 2D material deposited on a quartz plate). The sample is scanned along the waist of the beam (in the *z*-axis) in order to change the field intensity on the surface of the material.

The power in both arms is measured by a dual-channel power meter and afterward compared in order to calculate the saturable absorption curve.

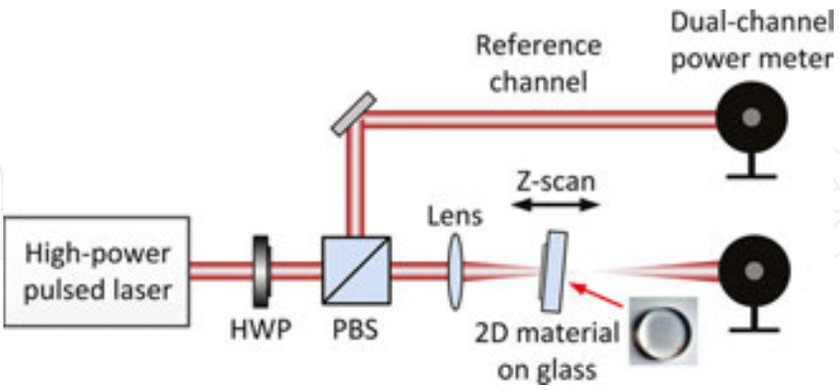

Figure 6. Power-dependent transmission measurement of a saturable absorber in free-space configuration.

In the case of fiber-based saturable absorbers (e.g., 2D material deposited on connectors or tapered fibers/D-shaped fibers), a modified version of the setup needs to be used. The schematic of an all-fiber power-dependent transmission experiment is depicted in **Figure 7**. Here, the power incident on the sample might tune with the use of a variable optical attenuator (VOA). The beam from the pump laser is also divided into two parts, but this time using a fiber coupler with defined coupling ratio, e.g., 50%/50%. Again, after passing through the absorber, the power is measured and compared with the reference channel.

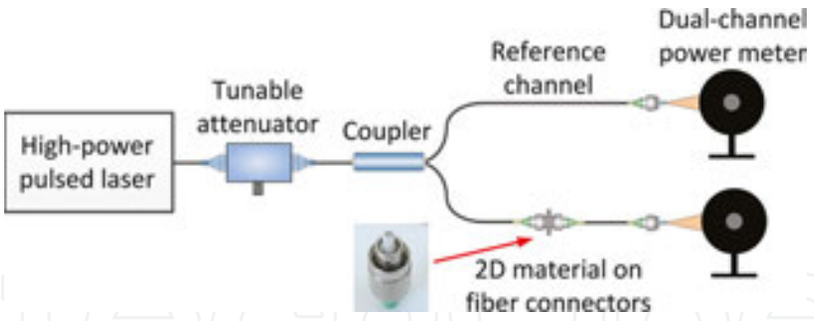

Figure 7. Power-dependent transmission measurement of a saturable absorber in all-fiber configuration.

3. Mode locking of lasers using graphene

3.1. Graphene

Graphene, one of the allotropes of carbon, is commonly described as a "wonderful material", thanks to its unique electronic properties and a great number of possible applications. Besides the application in pulsed lasers, graphene was successfully used in many optoelectronic devices, such as photodetectors [53], modulators [54], polarizers [55], sensors [56], and solar

cells [57]. The lack of the band gap in pristine graphene [58] might generally be unwanted in some electronic applications, but makes it extremely useful in photonics. Thanks to this unique property, graphene is characterized by a constant absorption coefficient in a wide spectral range. In consequence, it might act as a saturable absorber in lasers operating at different wavelengths. The historically first lasers mode-locked with graphene were developed in 2009 independently by the groups from Singapore and United Kingdom [16, 17]. Shortly after those reports, a number of papers appeared, demonstrating novel concepts of ultrafast lasers utilizing various forms of graphene. In this section, the unique optical properties of graphene will be discussed. The recent experimental results reported in the literature are described and compared.

3.2. Saturable absorption of graphene

The process of saturable absorption in a graphene was extensively studied by researchers in the recent years [59–61]. The process is schematically explained in **Figure 8**. A single graphene layer absorbs approximately a 2.3% fraction of the incident light [62]. The illumination causes excitation of the electrons from the valence band to the conduction band. After a very short relaxation time, these electrons cool down to a Fermi–Dirac distribution (step 2). After further illumination with high intensity light, the energy states in both bands fill, which blocks further absorption (Pauli blocking), and the saturable absorber bleaches [16, 61]. Graphene is characterized by a fast 70 – 150 fs relaxation transient, followed by a slower relaxation process in the 0.5 – 2.0 ps range, which was confirmed by pump-probe measurements [59, 60].

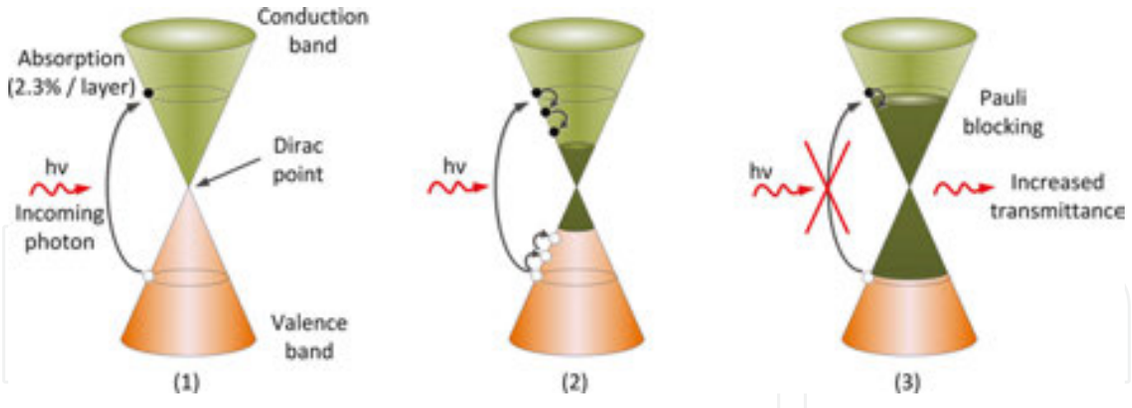

Figure 8. Saturable absorption in graphene [16, 59–61]. Light absorption and excitation of carriers (1), electrons cool down to a Fermi–Dirac distribution (2), and Pauli blocking (3).

As mentioned previously, a single layer of graphene absorbs approximately 2.3% of incident low intensity light. This absorption coefficient remains constant over a broad bandwidth, ranging from the visible to the mid-infrared [63]. However, the saturable absorption (i.e., the modulation depth) is slightly wavelength dependent. **Table 1** summarizes the experimentally obtained values of modulation depth, nonsaturable loss, and saturation fluence of monolayer graphene measured at four different wavelengths. It can be seen that the modulation depth is

the highest at shortest wavelength (800 nm) and drops quite rapidly with increased pump wavelength (0.5% at 1500 nm).

λ[nm]	ΔT [%]	α_{NS} [%]	F_{sat} [μJ/cm²]	Ref.
800	1.8	< 0.9	66.5	[20]
1040	0.75	1.59	50	[18]
1250	0.54	1.61	14.5	[64]
1500	0.5	1.9	14	[19]

Table 1. Summary of the experimentally obtained modulation depth value of monolayer graphene at different wavelengths.

An exemplary measurement of the nonlinear transmission through a CVD-grown monolayer of graphene deposited on a glass window is plotted in **Figure 9**. The curve was obtained using an experimental setup as depicted in **Figure 6**, with a 80-fs fiber laser operating at 1560 nm as an excitation source.

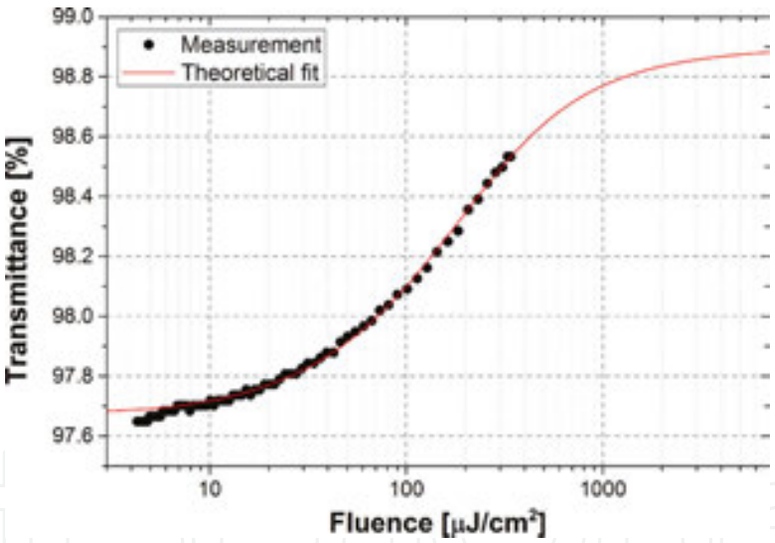

Figure 9. Measurement of saturable absorption in monolayer graphene.

Since graphene is considered as a fast saturable absorber (which is determined by its short relaxation time), its nonlinear transmission is described by different, more complex formula than the presented previously (Eq. (1)), valid for fast SAs [65, 66]:

$$T(F) = \frac{\Delta T}{\sqrt{\frac{F}{F_{sat}} + \left(\frac{F}{F_{sat}}\right)^2}} atanh\left(\sqrt{\frac{F}{F_{sat} + F}}\right) + (1 - \alpha_{NS}) \tag{2}$$

where ΔT denotes the modulation depth. The theoretical fit (solid red line in **Figure 9**) was calculated using the following parameters: F_{sat} = 105 μJ/cm^2, α_{NS} = 1.1%, and ΔT = 1.24%. The theoretical curve fits very well the experimental data; however, it can be seen that the sample was not fully saturated due to insufficient pump power.

3.3. Controlling the modulation depth of graphene-based saturable absorbers

As shown in the previous section, the modulation depth of a single graphene layer at the two most popular fiber laser wavelengths (1 and 1.55 μm) is quite small, at the level of 1%. Typically, in the case of fiber lasers, such modulation depth is insufficient to initiate stable mode locking and generate ultrashort optical pulses. It is therefore necessary to increase the modulation depth of a graphene-based saturable absorber. This might be done by scaling the number of graphene layers in the SA device. What is also important, the modulation depth is a critical parameter which determines the behavior of a laser. The influence of the modulation depth of the saturable absorber on the performance of mode-locked lasers was already extensively investigated numerically and experimentally. As an example, the study of Sobon et al. [67] has revealed that large numbers of graphene layers are required to achieve optimal performance for subpicosecond mode-locked operation of an Er- and Tm-doped laser. Unfortunately, increasing the number of layers does not only change the modulation depth, but causes also an increase of nonsaturable losses, which are usually unwanted in fiber lasers.

The optical transmittance of multilayer graphene was investigated by Zhu et al. They have derived a simplified formula, which describes the transmittance as a function of number of layers [68]:

$$T(N) = \left(1 + \frac{1.13 \cdot \pi\alpha N}{2}\right)^{-2} \tag{3}$$

where N denotes the number of layers and α is the fine-structure constant revealed by Nair et al. [62] (≈1/137). However, this formula is valid only for multilayer graphene with defined stacking sequence (e.g., ABA or ABC). Such ordered structure might be achieved, e.g., in a CVD growth process on nickel (Ni) substrate [68]. This formula takes into account the interactions between the adjacent layers, which are present only when the graphene layers are properly stacked.

In the case of undetermined stacking, when, e.g., the graphene layers were grown separately and afterward stacked together, and there are no inter-layer interactions, a different formula needs to be used to calculate the transmittance:

$$T(N) = (1 - \pi\alpha)^N \tag{4}$$

The passage of a laser beam through such a multilayer graphene stack is illustrated in **Figure 10**. The transmittance vs. number of layers curve calculated using both formulas is plotted in **Figure 11**, together with experimental data obtained in [67].

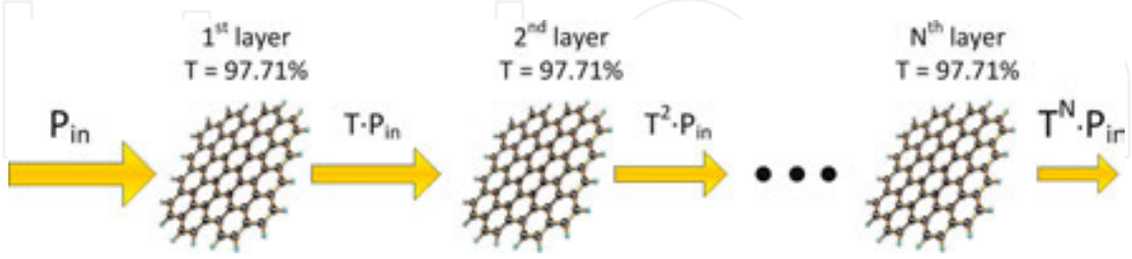

Figure 10. Light absorption in multilayer graphene without any interaction between the layers.

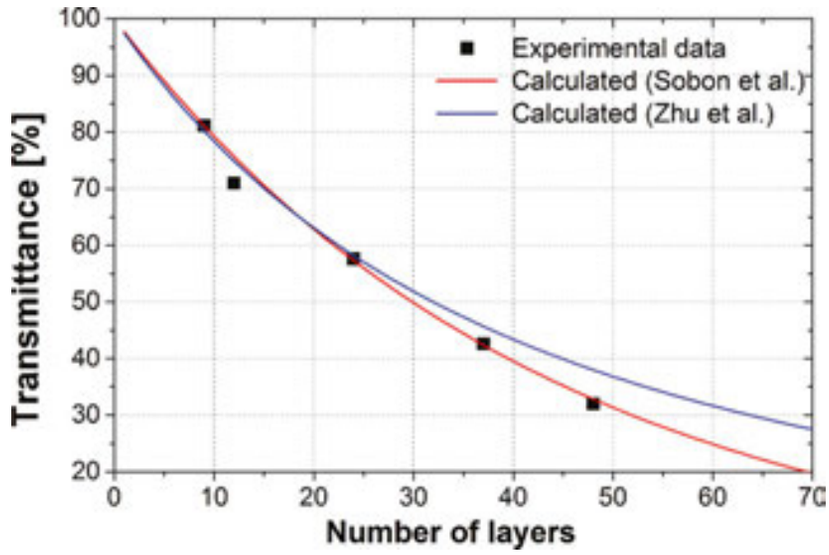

Figure 11. Optical transmittance of multilayer graphene: calculated from formula (1) (red line, no interaction between layers), calculated from formula (2) (blue line, including layer interactions), and measured using multilayer graphene (dotted line) [67].

As mentioned before, the modulation depth of graphene strongly depends on the number of layers. This allows to fabricate a proper saturable absorber to fulfill the requirements of a designed mode-locked laser. For example, dispersion-managed lasers (e.g., dissipative soliton lasers or stretched-pulse lasers) require much higher modulation depths than soliton lasers [69]. **Figure 12** shows the examples of nonlinear transmission curves of saturable absorbers containing 9, 12, 24, and 37 graphene layers [67]. It can be easily seen that the modulation depth increases with the growing number of layers. It starts from 3% for 9 layers, up to 7.5% for 37 layers.

http://dx.doi.org/10.5772/63336

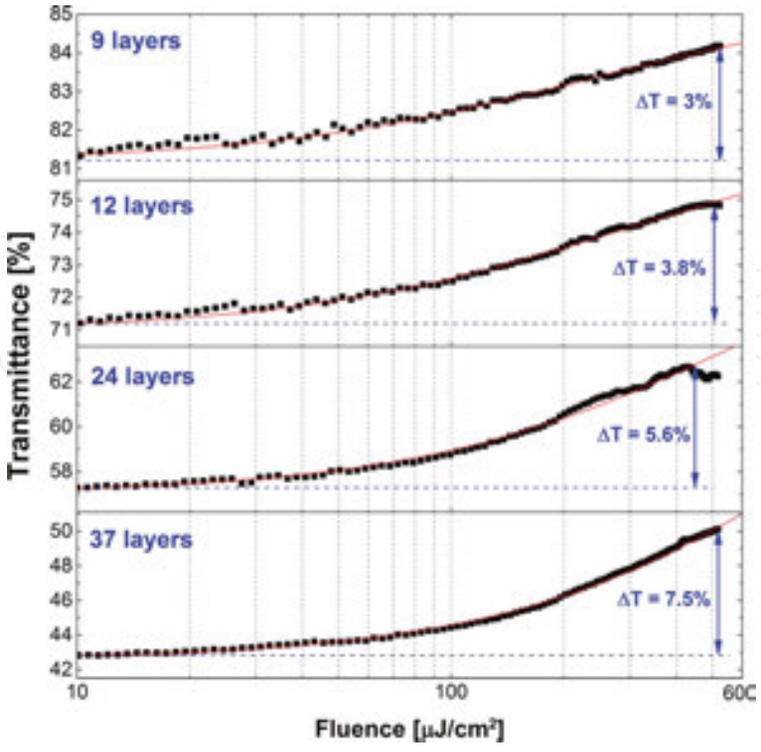

Figure 12. Nonlinear transmission curves of saturable absorbers containing 9, 12, 24, and 37 graphene layers.

3.4. Pulsed fiber lasers with graphene

The broadband saturable absorption of graphene makes this material an universal SA for different types of lasers. It has been already shown that the same graphene SA can provide mode locking in Yb-, Er-, and Tm-doped lasers [70], or can also synchronize and phase-lock two lasers simultaneously [71, 72].

Figure 13 shows the examples of three fiber lasers: Yb- (a), Er- (b) and Tm-doped (c) mode-locked with multilayer graphene composite. In the figure, each laser setup is depicted with its corresponding optical spectrum (e–g). All lasers were based on fully fiberized ring resonators and they utilized CVD-grown multilayer graphene immersed in a PMMA polymer support [73]. The Yb-doped oscillator consists of a segment of active fiber, an isolator, an output coupler (with 40/60% coupling ratio), a band-pass filter (BPF) with 2 nm FWHM, a polarization controller (PC), a 976 nm/1064 nm wavelength division multiplexer (WDM) and the saturable absorber. The laser was pumped by a 976 nm laser diode. Due to the normal dispersion of all fibers used in the cavity, a BPF is necessary to obtain dissipative soliton operation [74]. With the use of 48 layers of graphene in the SA, the laser generated pulses centered at 1059 nm and around 1.5 nm bandwidth and 17.1 MHz repetition frequency.

The Er-doped fiber laser shown in **Figure 13(b)** was realized in a simplified configuration, with the use of a hybrid component comprising an 10% output coupler (OC), a WDM and an isolator (ISO) in one integrated device. All fibers and components were polarization maintaining (PM), so there was no need to use a PC to initiate the mode locking. The optical spectrum generated

with the use of 32 layers of graphene is depicted in **Figure 13(e)**. It is centered at 1561 nm and has an FWHM of 20 nm, whereas the repetition rate was 100 MHz. The Tm-doped fiber laser was designed analogously to the Er-doped laser, but in this case the cavity was not all-PM, so the laser needs polarization alignment to initiate the mode locking. The oscillator is pumped at 1566 nm wavelength using a laser diode, beforehand amplified in an Erbium-doped fiber amplifier (EDFA). In this case, 12 layers of graphene were sufficient to support stable mode locking at 1968 nm with 10 nm of bandwidth (**Figure 13f**) and 100.25 MHz repetition frequency.

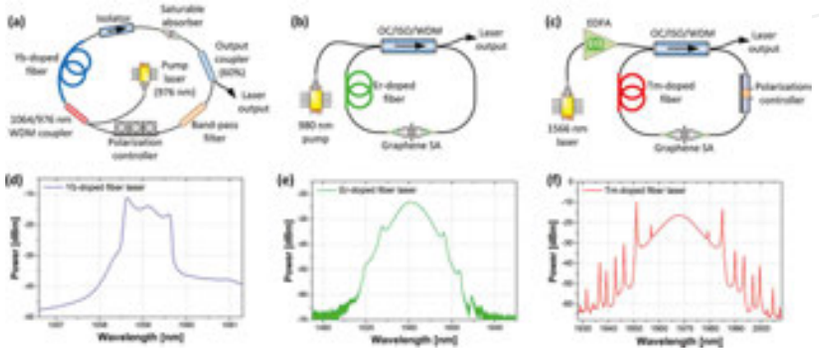

Figure 13. Fiber lasers operating at 1 μm (a), 1.55 μm (b), and 1.97 μm (c), and the corresponding optical spectra generated by those lasers (d, e, f).

3.5. Graphene-based ultrafast lasers – literature examples

3.5.1. Solid-state lasers

Efficient mode locking of solid-state lasers (SSLs) with the use of real saturable absorbers is quite challenging. The gain of an active medium (bulk crystal) is not as large as in fiber lasers, and in addition, the free-space resonator needs to be carefully aligned. Also the losses introduced by the SA should be possibly small. This is why most of the graphene-based SSLs utilize monolayer or bi-layer graphene. Up till now, mode locking of SSLs ranging from 532 to 2500 nm has been demonstrated [75, 76].

As an example, Baek et al. [20] demonstrated a Ti:Sapphire laser mode-locked with monolayer graphene. The laser generated 63 fs pulses at 800 nm central wavelength. There were also several reports on lasers operating around 1 μm wavelength [27–29]. The most prominent result was obtained by Ma et al. [29]. The authors have demonstrated stable 30 fs pulses centered at 1068 nm from diode pumped Yb:$CaYAlO_4$ laser by using high-quality CVD monolayer graphene as saturable absorber. These are the shortest pulses ever reported from graphene mode-locked lasers.

Broadband saturable absorption of graphene enables to achieve ultrashort pulse generation also in the mid infrared region. For example, Ma et al. [77] demonstrated a SSL based on a Tm-doped calcium lithium niobium gallium garnet (Tm:CLNGG) crystal, generating 729 fs pulses

at 2018 nm. The SA was formed by transferring CVD-grown, high-quality, and large-area graphene on a highly reflective plane mirror. Later, Cizmeciyan et al. [76] further extended the spectral coverage of graphene-based lasers by using a Cr:ZnSe crystal. High-quality monolayer graphene transferred on a CaF_2 windows enabled generation of 232 fs pulses at 2500 nm wavelength.

3.5.2. Ytterbium-doped fiber lasers

Mode locking of Yb-doped fiber lasers using real saturable absorbers might be challenging, mostly due to the fact that such oscillators are operated in the all-normal dispersion regime. The dispersion of standard single-mode fibers is normal for wavelengths shorter than ~1300 nm. Thus, a typical Yb-doped laser built from standard components will be characterized by a positive net group delay dispersion (GDD). This implies dissipative soliton operation of such laser. In order to generate a dissipative soliton, several conditions must be fulfilled [78]. The saturable absorber needs to have sufficient modulation depth in order to imitate and maintain the mode locking. In the case of graphene, it implies the usage of multilayer composites. Moreover, dissipative solitons are characterized by a quite large pulse energy, significantly larger than those achieved in conventional soliton lasers (e.g., Er- or Tm-doped). Optical damage of the SA might be a serious issue which precludes mode locking in Yb-doped fiber lasers.

Up to date, there were only few graphene-based, dissipative soliton Yb-doped fiber lasers reported [70, 79–82]. In all cases, the generated optical spectra were narrower than 2 nm. The broadest spectrum of 1.3 nm was achieved by Zhao et al. [79]. The obtained pulse duration was 580 ps. Such long pulse durations originates from the giant chirp, which is a consequence of the large normal dispersion of the cavity. Usually, dissipative soliton pulses from all-normal dispersion (ANDi) lasers are compressible almost to the transform-limited value [83, 84]. Nevertheless, the performance of the graphene-based YDFLs is far worse than of YDFLs utilizing other mode-locking techniques, such as NOLM/NALM, SESAM, or NPR, where broadband spectra with large pulse energies are achieved [85–87].

3.5.3. Erbium-doped fiber lasers

Erbium-doped fiber lasers are obviously the most popular constructions among all fiber lasers, thanks to the wide availability of cost-effective components for the telecom industry (couplers, isolators, multiplexers, photodiodes, etc.). The dispersion of standard optical fibers is anomalous at 1.55 μm, which implies soliton-type operation of a typical laser (without any dispersion compensation). Such lasers are quite easy to build in all-fiber configuration, without the necessity of using any free-space bulk components.

The first reported graphene-based fiber lasers back in 2009 were Er-doped fiber lasers [16, 17]. Shortly after those reports, a number of papers appeared, demonstrating novel concepts and ultrafast laser setups utilizing various forms of graphene. The shortest ever reported pulse generated from an Er-doped graphene-based fiber laser was 88 fs reported by Sotor et al. [88] in 2015. For a quite long time (over 4 years) the "world record" was held by Popa et al. (174

fs) [63]. In 2014, Tarka et al. [89] reported generation of 168 fs pulses. Both lasers (from [89] and [63]) were characterized by similar cavity design and similar saturable absorber (graphene obtained via LPE), with quite low modulation depth (2.6 and 2.0%). In both cases the pulse duration was also comparable (168 and 174 fs). The significant improvement in terms of pulse duration was possible not only by proper dispersion management, but mainly by increasing of the SA modulation depth to 11% [88]. The parameters of the three lasers with shortest reported pulses are summarized in **Table 2**.

Author/Group	Pulse duration	FWHM bandwidth	Cavity net dispersion	Saturable absorber type	SA mod. depth	Ref.
1J. Sotor et al. / Wroclaw Univ. of Technology	88 fs	48 nm	Balanced (~-0.0015 ps^2)	Multilayer CVD-graphene/PMMA	11%	[88]
2J. Tarka et al. / Wroclaw Univ. of Technology	168 fs	15.2 nm	Anomalous	LPE graphene in chitosan	2.6%	[89]
3D. Popa et al. / Cambridge Univ.	174 fs	15.6 nm	Balanced (~-0.05 ps^2)	LPE graphene in Polivinyl alcohol (PVA)	2%	[63]

Table 2. Summarized parameters of three graphene-based lasers emitting the shortest pulses.

3.5.4. Thulium-doped fiber lasers

Thulium-doped fiber lasers operating in the 1.9–2.0 μm are currently considered as one of the most important branches of laser technology [90, 91]. The number of applications of such lasers rapidly grows.

Pulsed Tm-doped fiber lasers are suitable for use in many surgical and dermatological procedures. Due to strong absorption of the 1.9–2.0 μm radiation in water, heating of only small areas of human tissues is achieved. The light penetration into the tissue is at the level of microns, which allows precise cutting. In addition, bleeding is suppressed by coagulation [92].

The second application, where Tm-doped fiber lasers might be used is laser spectroscopy, e.g., remote detection of air pollutants. The 1.9–2.0 μm spectral region contains multiple absorption lines of several molecules, especially two harmful greenhouse gases: carbon dioxide (CO_2) and nitrous oxide (N_2O). Carbon dioxide is the primary greenhouse gas that is contributing to recent climate change. It is absorbed and emitted naturally as part of the carbon cycle (e.g., animal and plant respiration, volcanic eruptions, ocean-atmosphere exchange), but also human activities strongly contribute to the global emission of CO_2 (e.g., burning of fossil fuels) [93]. Nitrous oxide is also a major greenhouse gas and air pollutant. The N_2O molecules stay in the atmosphere for an average of 120 years before being removed by a sink or destroyed through chemical reactions. Globally, about 40% of total N_2O emissions come from human activities [94]. Nitrous oxide is emitted from agriculture (when nitrogen is added to the soil

through the use of synthetic fertilizers), transportation (from burning of fuel), and industry activities (e.g., production of synthetic materials). It is predicted that N_2O emissions are going to increase by 5% between 2005 and 2020, driven largely by increases in emissions from agricultural activities [93–95].

Up to date there were only few reports on graphene-based Tm-doped fiber lasers. The first mode-locked TDFL was reported by Zhang et al. [96] in 2012. The authors have achieved 3.6 ps pulses at 1.94 μm. The laser was using chemically exfoliated graphene (via LPE method) dispersed in PVA host. Later, Wang et al. [97] demonstrated a TDFL emitting 2.1 ps pulses, based also on graphene exfoliated by ultrasonic method (dispersed in dimethyloformamide). In 2013, Sobon et al. [98] reported an all-fiber Tm-doped laser which generated 1.2 ps pulses at 1884 nm, using a CVD-graphene/PMMA composite. Improvements in the graphene technology and careful cavity optimization allowed the same authors to further shorten the pulse almost twice (654 fs at 1940 nm [73]). An interesting concept of a Tm/Ho-doped fiber laser was presented by Jung et al. [49]. The oscillator was mode-locked by a side-polished (D-shaped) fiber with deposited graphene oxide. Unfortunately, the pulse duration directly from the oscillator was unknown, due to insufficient output power to perform an autocorrelation measurement [49]. Later, the first polarization maintaining laser was demonstrated. The oscillator was capable of generating 603 fs pulses at 1876 nm [99]. The same group also reported chirped pulse amplification (CPA) of a Tm-doped oscillator in a fully fiberized design, achieving 260 fs pulses with more than 1 nJ energy at 1970 nm [100].

4. Other low-dimensional materials as saturable absorbers

4.1. Topological insulators

Among all the identified topological insulators, three have found very much attention by the photonics community: bismuth telluride (Bi_2Te_3), bismuth selenide (Bi_2Se_3) and antimony telluride (Sb_2Te_3). Carrier recombination mechanism in those materials was already investigated using time-resolved and angle-resolved photoelectron spectroscopy (tr-ARPES) [101–104], confirming the presence of surface metallic states.

The first mode-locked fiber laser incorporating a TI-based saturable absorber was proposed by Zhao et al. [22]. The oscillator emitted 1.21 ps pulses at 1558 nm with the use of Bi_2Te_3 TI. Further studies on the third-order nonlinear properties of Bi_2Te_3 performed by the same group revealed that the material might exhibit modulation depth up to 61.2% and possesses a very high third-order nonlinear refractive index, at the level of 10^{-14} m^2/W [105]. The most prominent and important research results on TI-based lasers include: the first demonstration of a Bi_2Se_3-based fiber laser [106], the first demonstration of harmonic mode locking with Bi_2Te_3 [107], first demonstration of the usage of Sb_2Te_3 topological insulator for mode locking [32], harmonic mode locking with Sb_2Te_3 [108], or development of TI-polymer composites [33]. The shortest pulse generated with a TI-based saturable absorber was reported in 2016 by Liu et al. [47]. The oscillator incorporated Sb_2Te_3 TI deposited on a tapered fiber and delivered 70 fs pulses at 1542 nm wavelength, whose 3 dB spectral width is 63 nm with a repetition rate of 95.4 MHz.

However, the mode locking was not truly SA based—the cavity contained an additional polarizer and wave-plates. Thus, the mode locking was a result of a hybrid combination of saturable absorption and NPR. The shortest pulses achieved directly from an oscillator mode-locked only by a TI-based SA were 128 fs [48].

4.2. Transition metal dichalcogenides

Transition metal dichalcogenides are in general characterized by the chemical formula MX_2, where M is a transition metal, e.g., molybdenum (Mo) or tungsten (W), and X is a group VI element: sulfur (S), selenium (Se), or tellurium (Te). Those materials were already investigated in the late 1960s of the twentieth century [109]. The general interest in TMDCs was renewed after the great success of graphene. Materials as such as MoS_2, $MoSe_2$, WS_2, WTe_2, $MoTe_2$, and WSe_2 are currently extensively investigated, since they allow applications as transistors, photodetectors, and optoelectronic devices [110]. In contrast to graphene, TMDCs are characterized by a band gap, which varies significantly with the material thickness [111].

The first TMDC material used as SA in lasers was molybdenum disulfide. The saturable absorption effect in MoS_2 nanosheets was already investigated in 2013 [112]. Less than one year after this discovery, Zhang et al. [34] demonstrated the first laser mode-locked with the use of MoS_2. The Yb-doped fiber laser generated stable pulses centered at 1054.3 nm, with a 3-dB spectral bandwidth of 2.7 nm and duration of 800 ps. Later, the same group has demonstrated ultrashort pulse generation from an Er-doped fiber laser mode-locked with MoS_2-based saturable absorber [35]. The laser generated 710 fs pulses centered at 1569.5 nm wavelength with a repetition rate of 12.09 MHz. Wavelength-tunable operation of a MoS_2-based fiber laser in a very broad spectral range was reported by Zhang et al. [113]. The demonstrated laser utilized a PVA-MoS_2 saturable absorber and enabled continuous tuning from 1535 to 1565 nm. Molybdenum disulfide can be also used in combination with tapered fibers. For example, Du et al. [46] demonstrated an Yb-doped fiber laser which generated dissipative solitons at 1042.6 nm with pulse duration of 656 ps and a repetition rate of 6.74 MHz. Also a harmonically mode-locked Er-doped laser incorporating a microfiber-based MoS_2 SA was reported [114]. Very recently, Wu et al. [115] demonstrated a reflective MoS_2 saturable absorber for a short-cavity Er-doped fiber laser. They have achieved 606 fs pulses at 1556.3 nm with 463 MHz repetition rate.

The saturable absorption effect was also confirmed for other TMDCs [116], but up to date, probably not all of them were used as mode-lockers in lasers. Recently WS_2 has found attention of the ultrafast laser community. Lasers operating at 1.03 μm [117], 1.55 μm [118, 119], and 1.94 μm [41] were already reported with pulse durations down to 595 fs [119].

4.3. Black phosphorus

Similarly to TMDCs, black phosphorus is a material which was once on interest of the physics community (in the 1980s and 1990s of the twentieth century [120, 121]), and was "rediscovered" in the recent years after the great success of other 2D materials.

http://dx.doi.org/10.5772/63336

It has a graphene-like layered structure, in which the layers are bound with van der Walls forces [122, 123]. Mechanical exfoliation of black phosphorus leads to obtaining a single-layer 2D material called phosphorene [121–124] (analogously to "graphene"). Similarly to TMDCs, the energy band gap of BP scales with the number of layers. It might be tuned from approx. 1.5 eV for monolayer phosphorene up to ~0.3 eV for bulk black phosphorus [125]. Up till now, the broadband nonlinear optical response of BP has been confirmed at wavelengths ranging from of 400 to 1930 nm [126, 127].

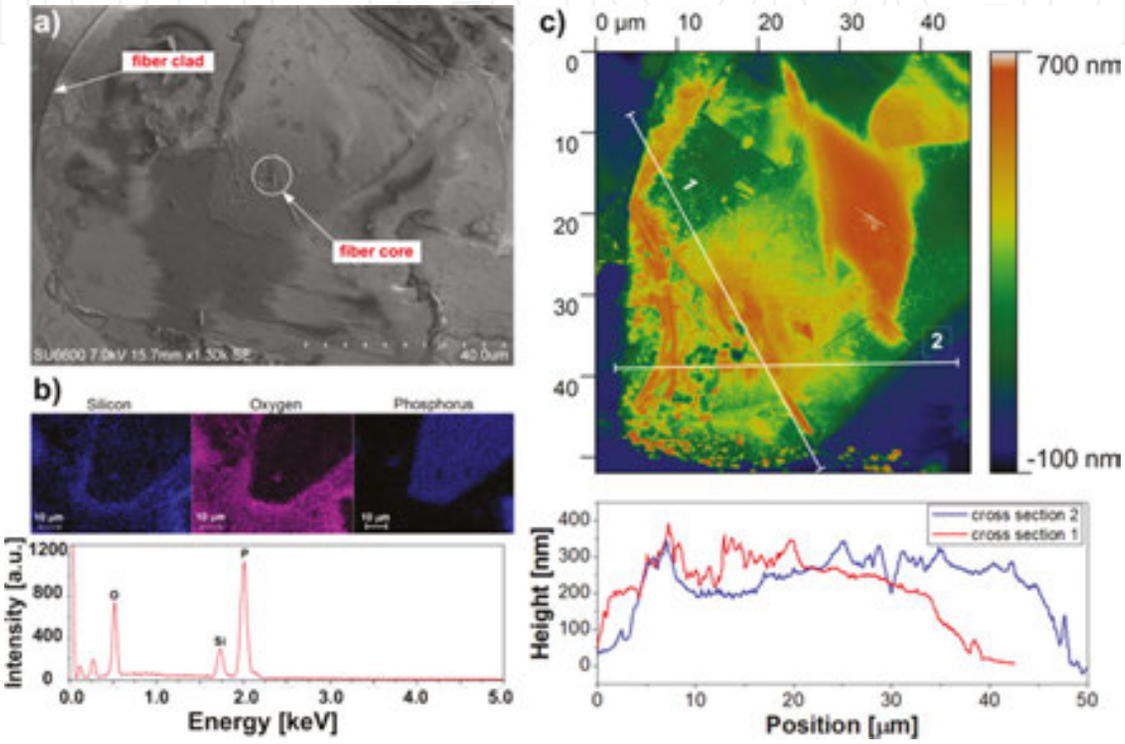

Figure 14. Characterization of the mechanically exfoliated BP layers transferred onto an optical fiber: (a) SEM image with marked fiber clad and core, (b) EDX spectroscopy data, (c) AFM image of the core area, and (d) cross section through the fiber core area indicating approx. 200–300 nm height of the BP flake on the core.

The first report on the usage of BP as a saturable absorber in a laser was posted on arXiv in 2015 [128]. Mode locking at both 1.55 and 1.9 µm wavelengths was reported. In both lasers, the BP layers were exfoliated mechanically from bulk material using an adhesive tape. Afterward, a ~300 nm thick layer was transferred onto a fiber connector, and connected with another one, just like shown in **Figure 14**. A scanning electron microscope (SEM) image of the fiber tip (with marked core and cladding of the fiber) with deposited BP layer is shown in **Figure 14(a)** [36]. The composition of the transferred layer onto the fiber core area was confirmed by energy-dispersive X-ray spectroscopy (EDX). The analysis of the spectroscopy data is shown in the inset of **Figure 14**. It confirms that the transferred material is black phosphorus (the Si and O peaks originate from the optical fiber). The atomic force microscope (AFM) measurement confirmed the average thickness of the layer at the level of 250–300 nm (**Figure 14b**).

The performance of the Tm-doped fiber laser mode-locked with the described BP-based saturable absorber is depicted in **Figure 15**. The laser generated soliton-shaped optical spectra centered at 1910 nm with 5.8 nm of FWHM bandwidth (a), which corresponded to a 739 fs pulse (b). It is worth mentioning that the authors claimed a high damage threshold of the BP layers. The laser was pumped with relatively high power (up to 400 mW) and the SA was not damaged or degraded during any of the performed experiments [37].

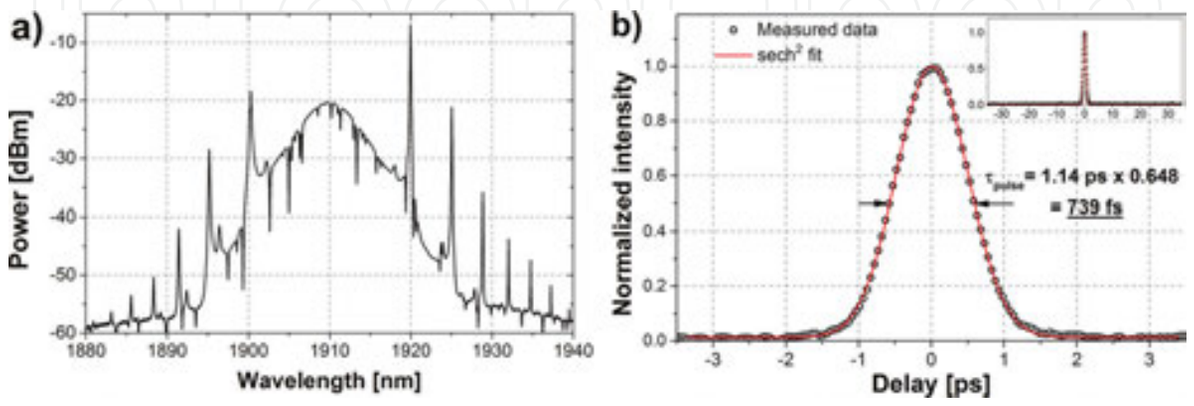

Figure 15. Optical spectrum generated by the BP mode-locked Tm-doped laser (a) and the autocorrelation trace of the emitted 739 fs pulse (b).

Black phosphorus in form of nanopalettes (NPs) was also used in combination with microfibers for evanescent field interaction. In their work, Yu et al. [129] reported that the SA had a modulation depth of 9.8% measured at 1.93 μm. A stable mode-locking operation at 1898 nm was achieved with a pulse width of 1.58 ps and a fundamental repetition rate of 19.2 MHz.

Similarly to graphene, BP is also suitable for operation in the midinfrared. In 2016, Wang et al. [130] demonstrated the first Cr:ZnSe laser incorporating BP as saturable absorber. However, the laser was not mode-locked but Q-switched. Generation of 189 ns pulses with average output power of 36 mW was obtained at 2.4 μm wavelength.

5. Summary and outlook

In summary, the recent most important advances in the field of ultrashort-pulsed lasers utilizing two-dimensional materials have been presented. A group of 2D materials, such as graphene, topological insulators, and transition metal dichalcogenides, have unambiguously revolutionized the field of mode-locked fiber-based and solid-state lasers. The discovery of unique optical properties of graphene has initiated an extremely fast progress in the science of two-dimensional nanomaterials, which strongly contributed to the development of novel ultrafast laser sources. It is evident that the interest in 2D material-based photonics will not slow down in the next years.

Acknowledgements

The author acknowledges the help and support from the members of the Laser & Fiber Electronics Group, especially Jaroslaw Sotor, Jakub Boguslawski, Maciej Kowalczyk, Jan Tarka, Karol Krzempek, and Krzysztof M. Abramski. The author also like to kindly thank the collaborators from the Institute of Electronic Materials Technology (Warsaw, Poland) for their excellent work on graphene fabrication and characterization. The research presented in this chapter was supported by the National Science Centre (NCN, Poland) under grants no. DEC-2013/11/D/ST7/03138 and DEC-2014/13/B/ST7/01699, and by the statutory funds of the Chair of EM Field Theory, Electronic Circuits and Optoelectronics (grant no. S50044).

Author details

Grzegorz Sobon

Address all correspondence to: grzegorz.sobon@pwr.edu.pl

Laser and Fiber Electronics Group, Faculty of Electronics, Wrocław University of Technology, Wrocław, Poland

References

[1] Novoselov KS, Geim AK, Morozov SV, Jiang D, Zhang Y, Dubonos SV et al. Electric field effect in atomically thin carbon films. Science. 2004;306:666–669.

[2] Mamalis N. Femtosecond laser. The future of cataract surgery? J. Cataract Refract Surg. 2011;37:1177–1178.

[3] Gattass RR, Mazur E. Femtosecond laser micromachining in transparent materials. Nat Photonics. 2008;2:219–225.

[4] Ehlers P, Silander I, Wang J, Foltynowicz A, Axner O. Fiber-laser-based noise-immune cavity-enhanced optical heterodyne molecular spectrometry incorporating an optical circulator. Opt Lett. 2014;39:279–282.

[5] Kowzan G, Lee KF, Paradowska M, Borkowski M, Ablewski P, Wójtewicz S et al. Self-referenced, accurate and sensitive optical frequency comb spectroscopy with a virtually imaged phased array spectrometer. Opt Lett. 2016;41:974–977.

[6] Stehr D, Morris CM, Schmidt C, Sherwin MS. High-performance fiber-laser-based terahertz spectrometer. Opt Lett. 2010;35:3799–3801.

[7] Tang S, Liu J, Krasieva TB, Chen Z, Tromberg BJ. Developing compact multiphoton systems using femtosecond fiber lasers. J Biomed Opt. 2009;14:030508.

[8] Buczynski R, Bookey HT, Pysz D, Stepien R, Kujawa I, McCarthy JE et al. Supercontinuum generation up to 2.5 μm in photonic crystal fiber made of lead-bismuth-galate glass. Laser Phys Lett. 2010;7:666–672.

[9] Wilken T, Lo Curto G, Probst RA, Steinmetz T, Manescau A, Pasquini L et al. A spectrograph for exoplanet observations calibrated at the centimetre-per-second level. Nature. 2012;485:611–614.

[10] Ludlow AD, Boyd MM, Ye J, Peik E, Schmidt PO. Optical atomic clocks. Rev Mod Phys. 2015;87:637–701.

[11] Boyd RW. Nonlinear Optics. San Jose: Academic Press; 2003.

[12] Kärtner FX, Aus der Au J, Keller U. Mode-locking with slow and fast saturable absorbers—what's the difference?. IEEE J Sel Top Quant. 1998;4:159–168.

[13] Keller U, Weingarten KJ, Kärtner FX, Kopf D, Braun B, Jung ID et al. Semiconductor saturable absorber mirrors (SESAMs) for femtosecond to nanosecond pulse generation in solid-state lasers. IEEE J Sel Top Quant Electron. 1996;2:435–453.

[14] Okhotnikov O, Grudinin A, Pessa M. Ultra-fast fibre laser systems based on SESAM technology: new horizons and applications. New J Phys. 2004;6:177.

[15] Set SY, Yaguchi H, Tanaka Y, Jablonski M, Sakakibara Y, Rozhin A et al. Mode-locked fiber lasers based on a saturable absorber incorporating carbon nanotubes. In: Optical Fiber Communication Conference, 23–28 March 2003; Atlanta. Optical Society of America; 2003. p. PD44.

[16] Bao QL, Zhang H, Wang Y, Ni ZH, Shen ZX, Loh KP et al. Atomic layer graphene as saturable absorber for ultrafast pulsed laser. Adv Funct Mater. 2009;19:3077–3083.

[17] Hasan T, Sun Z, Wang F, Bonaccorso F, Tan PH, Rozhin AG et al. Nanotube–polymer composites for ultrafast photonics. Adv Mater. 2009;21:3874–3899.

[18] Ugolotti E, Schmidt A, Petrov V, Wan Kim J, Yeom D, Rotermund F et al. Graphene mode-locked femtosecond Yb:KLuW laser. Appl Phys Lett. 2012;101(16):161112

[19] Di Dio Cafiso SD, Ugolotti E, Schmidt A, Petrov V, Griebner U, Agnesi A, Cho WB, Jung BH, Rotermund F, Bae S, Hong BH, Reali G, Pirzio F. Sub-100-fs Cr:YAG laser mode-locked by monolayer graphene saturable absorber. Opt Lett. 2013;38;1745–1747.

[20] Baek I, Lee H, Bae S, Hong B, Ahn Y, Yeom D et al. Efficient mode-locking of sub-70-fs Ti:sapphire laser by graphene saturable absorber. Appl Phys Express. 2012;5(3):032701

[21] Sobon G, Sotor J, Pasternak I, Grodecki K, Paletko P, Strupinski W et al. Er-doped fiber laser mode-locked by CVD-graphene saturable absorber. J Lightwave Technol. 2012;30:2770–2775.

[22] Zhao C, Zhang H, Qi X, Chen Y, Wang Z, Wen S, Tang D. Ultra-short pulse generation by a topological insulator based saturable absorber," Appl Phys Lett. 2012;101:211106

[23] Xu J, Liu J, Wu S, Yang QH, Wang P. Graphene oxide mode-locked femtosecond erbium-doped fiber lasers. Opt Express. 2012;20:15474–15480.

[24] Xu J, Wu S, Li H, Liu J, Sun R, Tan F et al. Dissipative soliton generation from a graphene oxide mode-locked Er-doped fiber laser. Opt Express. 2012;20:23653.

[25] Cunning B, Brown C, Kielpinski D. Low-loss flake-graphene saturable absorber mirror for laser mode-locking at sub-200-fs pulse duration. Appl Phys Lett. 2011;99:261109.

[26] Lou F, Cui L, Li Y, Hou J, He J, Jia Z et al. High-efficiency femtosecond Yb:$Gd_3Al_{05}Ga_{45}O_{-12}$ mode-locked laser based on reduced graphene oxide. Opt Lett. 2013;38:4189.

[27] Xu J, Li X, Wu Y, Hao X, He J, Yang K. Graphene saturable absorber mirror for ultra-fast-pulse solid-state laser. Opt Lett. 2011;36(10):1948.

[28] Xu J, Li X, He J, Hao X, Wu Y, Yang Y et al. Performance of large-area few-layer graphene saturable absorber in femtosecond bulk laser. Appl Phys Lett. 2011;99(26):261107.

[29] Ma J, Huang H, Ning K, Xu X, Xie G, Qian L et al. Generation of 30 fs pulses from a diode-pumped graphene mode-locked Yb:$CaYAlO_4$ laser. Opt Lett. 2016;41:890.

[30] Bonaccorso F, Sun Z. Solution processing of graphene, topological insulators and other 2d crystals for ultrafast photonics. Opt Mater Express. 2014;4:63–78.

[31] Huang P, Lin S, Yeh C, Kuo H, Huang S, Lin G et al. Stable mode-locked fiber laser based on CVD fabricated graphene saturable absorber. Opt Express. 2012;20:2460.

[32] Sotor J, Sobon G, Macherzynski W, Paletko P, Grodecki K, Abramski K. Mode-locking in Er-doped fiber laser based on mechanically exfoliated Sb_2Te_3 saturable absorber. Opt Mater Express. 2013;4:1.

[33] Liu H, Zheng X, Liu M, Zhao N, Luo A, Luo Z et al. Femtosecond pulse generation from a topological insulator mode-locked fiber laser. Opt Express. 2014;22(6):6868.

[34] Zhang H, Lu S, Zheng J, Du J, Wen S, Tang D et al. Molybdenum disulfide (MoS_2) as a broadband saturable absorber for ultra-fast photonics. Opt Express. 2014;22:7249.

[35] Liu H, Luo A, Wang F, Tang R, Liu M, Luo Z et al. Femtosecond pulse erbium-doped fiber laser by a few-layer MoS_2 saturable absorber. Opt Lett. 2014;39:4591.

[36] Sotor J, Sobon G, Macherzynski W, Paletko P, Abramski K. Black phosphorus saturable absorber for ultrashort pulse generation. Appl Phys Lett. 2015;107:051108.

[37] Sotor J, Sobon G, Kowalczyk M, Macherzynski W, Paletko P, Abramski K. Ultrafast thulium-doped fiber laser mode locked with black phosphorus. Opt Lett. 2015;40:3885.

[38] Song Y, Yamashita S, Goh C, Set S. Carbon nanotube mode lockers with enhanced nonlinearity via evanescent field interaction in D-shaped fibers. Opt Lett. 2006;32:148.

[39] Song Y, Jang S, Han W, Bae M. Graphene mode-lockers for fiber lasers functioned with evanescent field interaction. Appl Phys Lett. 2010;96:051122.

[40] Sotor J, Sobon G, Grodecki K, Abramski K. Mode-locked erbium-doped fiber laser based on evanescent field interaction with Sb2Te3 topological insulator. Appl Phys Lett. 2014;104:251112.

[41] Jung M, Lee J, Park J, Koo J, Jhon Y, Lee J. Mode-locked, 1.94-μm, all-fiberized laser using WS_2-based evanescent field interaction. Opt Express. 2015;23:19996.

[42] Luo Z, Wang J, Zhou M, Xu H, Cai Z, Ye C. Multiwavelength mode-locked erbium-doped fiber laser based on the interaction of graphene and fiber-taper evanescent field. Laser Phys Lett. 2012;9:229–233.

[43] Wang J, Luo Z, Zhou M, Ye C, Fu H, Cai Z et al. Evanescent-Light Deposition of graphene onto tapered fibers for passive Q-switch and mode-locker. IEEE Photonics J. 2012;4:1295–1305.

[44] Kieu K, Mansuripur M. Femtosecond laser pulse generation with a fiber taper embedded in carbon nanotube/polymer composite. Opt Lett. 2007;32:2242.

[45] Kashiwagi K, Yamashita S. Deposition of carbon nanotubes around microfiber via evanascent light. Opt Express. 2009;17:18364.

[46] Du J, Wang Q, Jiang G, Xu C, Zhao C, Xiang Y et al. Ytterbium-doped fiber laser passively mode locked by few-layer molybdenum disulfide (MoS2) saturable absorber functioned with evanescent field interaction. Sci Rep. 2014;4:6346.

[47] Liu W, Pang L, Han H, Tian W, Chen H, Lei M et al. 70-fs mode-locked erbium-doped fiber laser with topological insulator. Sci Rep. 2016;5:19997.

[48] Sotor J, Sobon G, Abramski K. Sub-130 fs mode-locked Er-doped fiber laser based on topological insulator. Opt Express. 2014;22:13244.

[49] Jung M, Koo J, Park J, Song Y, Jhon Y, Lee K et al. Mode-locked pulse generation from an all-fiberized, Tm-Ho-codoped fiber laser incorporating a graphene oxide-deposited side-polished fiber. Opt Express. 2013;21:20062.

[50] Park N, Jeong H, Choi S, Kim M, Rotermund F, Yeom D. Monolayer graphene saturable absorbers with strongly enhanced evanescent-field interaction for ultrafast fiber laser mode-locking. Opt Express. 2015;23:19806.

[51] Bogusławski J, Soboń G, Zybała R, Mars K, Mikuła A, Abramski K et al. Investigation on pulse shaping in fiber laser hybrid mode-locked by Sb_2Te_3 saturable absorber. Opt Express. 2015;23:29014.

[52] Rusu M, Herda R, Kivistö S, Okhotnikov O. Fiber taper for dispersion management in a mode-locked ytterbium fiber laser. Opt Lett. 2006;31:2257.

[53] Mueller T, Xia F, Avouris P. Graphene photodetectors for high-speed optical communications. Nat Photonics. 2010;4:297–301.

[54] Liu M, Yin X, Ulin-Avila E, Geng B, Zentgraf T, Ju L et al. A graphene-based broadband optical modulator. Nature. 2011;474:64–67.

[55] Kim J, Choi C. Graphene-based polymer waveguide polarizer. Opt Express. 2012;20:3556.

[56] Shao Y, Wang J, Wu H, Liu J, Aksay IA, Lin Y. Graphene based electrochemical sensors and biosensors: a review. Electroanalysis. 2010;22:1027–1036.

[57] Wang X, Zhi L, Müllen K. Transparent, Conductive graphene electrodes for dye-sensitized solar cells. Nano Lett. 2008;8:323–327.

[58] Castro Neto A, Guinea F, Peres N, Novoselov K, Geim A. The electronic properties of graphene. Rev Modern Phys. 2009;81:109–162.

[59] Xing G, Guo H, Zhang X, Sum T, Huan C. The physics of ultrafast saturable absorption in graphene. Opt Express. 2010;18:4564.

[60] Newson R, Dean J, Schmidt B, van Driel H. Ultrafast carrier kinetics in exfoliated graphene and thin graphite films. Opt Express. 2009;17:2326.

[61] Dawlaty J, Shivaraman S, Chandrashekhar M, Spencer M, Rana F. Measurement of ultrafast carrier dynamics in epitaxial graphene. MRS Proc. 2008;1081.

[62] Nair R, Blake P, Grigorenko A, Novoselov K, Booth T, Stauber T et al. Fine structure constant defines visual transparency of graphene. Science 2008;320:1308–1308.

[63] Popa D, Sun Z, Torrisi F, Hasan T, Wang F, Ferrari A. Sub 200 fs pulse generation from a graphene mode-locked fiber laser. Appl Phys Lett. 2010;97:203106.

[64] Cho W, Kim J, Lee H, Bae S, Hong B, Choi S et al. High-quality, large-area monolayer graphene for efficient bulk laser mode-locking near 125 μm. Opt Lett. 2011;36:4089.

[65] Zaugg C, Sun Z, Wittwer V, Popa D, Milana S, Kulmala T et al. Ultrafast and widely tuneable vertical-external-cavity surface-emitting laser, mode-locked by a graphene-integrated distributed Bragg reflector. Opt Express. 2013;21:31548.

[66] Schibli T, Thoen E, Kärtner F, Ippen E. Suppression of Q-switched mode locking and break-up into multiple pulses by inverse saturable absorption. Appl Phys. B 2000;70:S41–S49.

[67] Sobon G, Sotor J, Pasternak I, Krajewska A, Strupinski W, Abramski K. Multilayer graphene-based saturable absorbers with scalable modulation depth for mode-locked Er- and Tm-doped fiber lasers. Opt Mater Express. 2015;5:2884.

[68] Zhu S, yuan S, Janssen G. Optical transmittance of multilayer graphene. EPL 2014;108:17007.

[69] Liu H, Chow K. Enhanced stability of dispersion-managed mode-locked fiber lasers with near-zero net cavity dispersion by high-contrast saturable absorbers. Opt Lett. 2013;39:150.

[70] Fu B, Hua Y, Xiao X, Zhu H, Sun Z, Yang C. Broadband graphene saturable absorber for pulsed fiber lasers at 1, 1.5, and 2 μm. IEEE J. Sel. Top. Quantum Electron. 2014;20:1100705.

[71] Sotor J, Sobon G, Pasternak I, Krajewska A, Strupinski W, Abramski K. Simultaneous mode-locking at 1565 nm and 1944 nm in fiber laser based on common graphene saturable absorber. Opt Express. 2013;21:18994.

[72] Sotor J, Sobon G, Tarka J, Pasternak I, Krajewska A, Strupinski W et al. Passive synchronization of erbium and thulium doped fiber mode-locked lasers enhanced by common graphene saturable absorber. Opt Express. 2014;22:5536.

[73] Sobon G. Mode-locking of fiber lasers using novel two-dimensional nanomaterials: graphene and topological insulators [Invited]. Photon Res. 2015;3:A56.

[74] Grelu P, Akhmediev N. Dissipative solitons for mode-locked lasers. Nat Photonics. 2012;6:84–92.

[75] Shi R, Bai Y, Qi M, Chen X, Wei H, Ren Z et al. A passively mode-locked intracavity frequency doubled Nd:YVO 4 femtosecond green laser based on graphene. Laser Phys Lett. 2013;11:025001.

[76] Cizmeciyan M, Kim J, Bae S, Hong B, Rotermund F, Sennaroglu A. Graphene mode-locked femtosecond Cr:ZnSe laser at 2500 nm. Opt Lett. 2013;38:341.

[77] Ma J, Xie G, Lv P, Gao W, Yuan P, Qian L et al. Graphene mode-locked femtosecond laser at 2 μm wavelength. Opt Lett. 2012;37:2085.

[78] Renninger W, Chong A, Wise F. Dissipative solitons in normal-dispersion fiber lasers. Phys. Rev. A 2008;77: 023814

[79] Zhao L, Tang D, Zhang H, Wu X, Bao Q, Loh K. Dissipative soliton operation of an ytterbium-doped fiber laser mode locked with atomic multilayer graphene. Opt Lett. 2010;35:3622.

[80] Liu J, Wei R, Xu X, Wang P. Mode-locked fiber laser with few-layer epitaxial graphene grown on 6H-SiC substrates. In: CLEO:2011 – Laser Applications to Photonic Applications 2011, 1–6 May 2011, Baltimore, USA; p. CMK3.

[81] Liu J, Wu S, Yang Q, Song Y, Wang Z, Wang P. 163 nJ graphene mode-locked Yb-doped fiber laser. In: CLEO:2011 – Laser Applications to Photonic Applications 2011; 1–6 May 2011; Baltimore, USA; p. JWA23.

[82] Li X, Wang Y, Wang Y, Zhang Y, Wu K, Shum P et al. All-normal-dispersion passively mode-locked Yb-doped fiber ring laser based on a graphene oxide saturable absorber. Laser Phys Lett. 2013;10:075108.

[83] Chong A, Buckley J, Renninger W, Wise F. All-normal-dispersion femtosecond fiber laser. Opt Express. 2006;14:10095.

[84] Chong A, Renninger W, Wise F. All-normal-dispersion femtosecond fiber laser with pulse energy above 20 nJ. Opt Lett. 2007;32:2408.

[85] Szczepanek J, Kardaś T, Michalska M, Radzewicz C, Stepanenko Y. Simple all-PM-fiber laser mode-locked with a nonlinear loop mirror. Opt Lett. 2015;40:3500.

[86] Chichkov N, Hapke C, Hausmann K, Theeg T, Wandt D, Morgner U et al. 05 μJ pulses from a giant-chirp ytterbium fiber oscillator. Opt Express. 2011;19:3647.

[87] Lecourt J, Duterte C, Narbonneau F, Kinet D, Hernandez Y, Giannone D. All-normal dispersion, all-fibered PM laser mode-locked by SESAM. Opt Express. 2012;20:11918.

[88] Sotor J, Pasternak I, Krajewska A, Strupinski W, Sobon G. Sub-90 fs a stretched-pulse mode-locked fiber laser based on a graphene saturable absorber. Opt Express. 2015;23:27503.

[89] Tarka J, Sobon G, Boguslawski J, Sotor J, Jagiello J, Aksienionek M et al. 168 fs pulse generation from graphene-chitosan mode-locked fiber laser. Opt Mater Express. 2014;4:1981.

[90] Hudson D. Invited paper: Short pulse generation in mid-IR fiber lasers. Opt Fiber Technol. 2014;20:631–641.

[91] Rudy C, Digonnet M, Byer R. Advances in 2-μm Tm-doped mode-locked fiber lasers. Opt Fiber Technol. 2014;20:642–649.

[92] Scholle K, Lamrini S, Koopmann P, Fuhrberg P. 2 μm laser sources and their possible applications. In: Frontiers in Guided Wave Optics and Optoelectronics. InTech; 2010.

[93] Inventory of U.S. Greenhouse Gas Emissions and Sinks: 1990–2011, EPA 430-R-13-001. U.S. Environmental Protection Agency; 2013.

[94] Anderson B, Bartlett K, Frolking S, Hayhoe K, Jenkins J, Salas W. Methane and Nitrous Oxide Emissions from Natural Sources. U.S. Environmental Protection Agency; Washington, DC, USA; 2010.

[95] Projected Greenhouse Gas Emissions. In: Fourth Climate Action Report to the UN Framework Convention on Climate Change. U.S. Department of State, Washington, DC, USA; 2007.

[96] Zhang M, Kelleher E, Torrisi F, Sun Z, Hasan T, Popa D et al. Tm-doped fiber laser mode-locked by graphene-polymer composite. Opt Express. 2012;20:25077.

[97] Wang Q, Chen T, Zhang B, Li M, Lu Y, Chen K. All-fiber passively mode-locked thulium-doped fiber ring laser using optically deposited graphene saturable absorbers. Appl Phys Lett. 2013;102:131117.

[98] Sobon G, Sotor J, Pasternak I, Krajewska A, Strupinski W, Abramski K. Thulium-doped all-fiber laser mode-locked by CVD-graphene/PMMA saturable absorber. Opt Express. 2013;21:12797.

[99] Sobon G, Sotor J, Pasternak I, Krajewska A, Strupinski W, Abramski K. All-polarization maintaining, graphene-based femtosecond Tm-doped all-fiber laser. Opt Express. 2015;23:9339.

[100] Sobon G, Sotor J, Pasternak I, Krajewska A, Strupinski W, Abramski K. 260 fs and 1 nJ pulse generation from a compact, mode-locked Tm-doped fiber laser. Opt Express. 2015;23:31446.

[101] Peng H, Dang W, Cao J, Chen Y, Wu D, Zheng W et al. Topological insulator nanostructures for near-infrared transparent flexible electrodes. Nat Chem. 2012;4:281–286.

[102] Hajlaoui M, Papalazarou E, Mauchain J, Lantz G, Moisan N, Boschetto D et al. Ultrafast surface carrier dynamics in the topological insulator Bi_2Te_3. Nano Lett. 2012;12:3532–3536.

[103] Kumar N, Ruzicka B, Butch N, Syers P, Kirshenbaum K, Paglione J et al. Spatially resolved femtosecond pump-probe study of topological insulator Bi_2Se_3. Phys. Rev. B 2011;83: 235306

[104] Hsieh D, Mahmood F, McIver J, Gardner D, Lee Y, Gedik N. Selective probing of photoinduced charge and spin dynamics in the bulk and surface of a topological insulator. Phys Rev Lett. 2011;107

[105] Lu S, Zhao C, Zou Y, Chen S, Chen Y, Li Y et al. Third order nonlinear optical property of Bi_2Se_3. Opt Express. 2013;21:2072.

[106] Zhao C, Zou Y, Chen Y, Wang Z, Lu S, Zhang H et al. Wavelength-tunable picosecond soliton fiber laser with topological insulator: Bi_2Se_3 as a mode locker. Opt Express. 2012;20:27888.

[107] Luo Z, Liu M, Liu H, Zheng X, Luo A, Zhao C et al. 2 GHz passively harmonic mode-locked fiber laser by a microfiber-based topological insulator saturable absorber. Opt Lett. 2013;38:5212.

[108] Sotor J, Sobon G, Macherzynski W, Abramski K. Harmonically mode-locked Er-doped fiber laser based on a Sb_2Te_3 topological insulator saturable absorber. Laser Phys Lett. 2014;11:055102.

[109] Wilson J, Yoffe A. The transition metal dichalcogenides discussion and interpretation of the observed optical, electrical and structural properties. Adv Phys. 1969;18:193–335.

[110] Wang Q, Kalantar-Zadeh K, Kis A, Coleman J, Strano M. Electronics and optoelectronics of two-dimensional transition metal dichalcogenides. Nat Nanotech 2012;7:699–712.

[111] Kumar A, Ahluwalia P. Electronic structure of transition metal dichalcogenides monolayers 1H-MX2 (M = Mo, W; X = S, Se, Te) from ab-initio theory: new direct band gap semiconductors. The European Physical Journal B 2012;85:186

[112] Wang K, Wang J, Fan J, Lotya M, O'Neill A, Fox D et al. Ultrafast saturable absorption of two-dimensional MoS_2 nanosheets. ACS Nano 2013;7:9260–9267.

[113] Zhang M, Howe R, Woodward R, Kelleher E, Torrisi F, Hu G et al. Solution processed MoS_2-PVA composite for sub-bandgap mode-locking of a wideband tunable ultrafast Er:fiber laser. Nano Res. 2015;8:1522–1534.

[114] Liu M, Zheng X, Qi Y, Liu H, Luo A, Luo Z et al. Microfiber-based few-layer MoS_2 saturable absorber for 2.5 GHz passively harmonic mode-locked fiber laser. Opt Express. 2014;22:22841.

[115] Wu K, Zhang X, Wang J, Chen J. 463-MHz fundamental mode-locked fiber laser based on few-layer MoS_2 saturable absorber. Opt Lett. 2015;40:1374.

[116] Mao D, Du B, Yang D, Zhang S, Wang Y, Zhang W et al. Nonlinear saturable absorption of liquid-exfoliated molybdenum/tungsten ditelluride nanosheets. Small. DOI: 10.1002/smll.201503348

[117] Guoyu H, Song Y, Li K, Dou Z, Tian J, Zhang X. Mode-locked ytterbium-doped fiber laser based on tungsten disulphide. Laser Phys Lett. 2015;12:125102.

[118] Mao D, Wang Y, Ma C, Han L, Jiang B, Gan X et al. WS_2 mode-locked ultrafast fiber laser. Sci Rep. 2015;5:7965.

[119] Wu K, Zhang X, Wang J, Li X, Chen J. WS_2 as a saturable absorber for ultrafast photonic applications of mode-locked and Q-switched lasers. Opt Express. 2015;23:11453.

[120] Nishii T, Maruyama Y, Inabe T, Shirotani I. Synthesis and characterization of black phosphorus intercalation compounds. Synth Met. 1987;18:559–564.

[121] Baba M, Nakamura Y, Takeda Y, Shibata K, Morita A, Koike Y et al. Hall effect and two-dimensional electron gas in black phosphorus. J Phys: Conden Matter. 1992;4:1535–1544.

[122] Xia F, Wang H, Jia Y. Rediscovering black phosphorus as an anisotropic layered material for optoelectronics and electronics. Nature Communications 2014;5:4458

[123] Liu H, Neal A, Zhu Z, Luo Z, Xu X, Tománek D et al. Phosphorene: an unexplored 2D semiconductor with a high hole mobility. ACS Nano. 2014;8:4033–4041.

[124] Cai Y, Zhang G, Zhang YW. Layer-dependent band alignment and work function of few-layer phosphorene. Sci. Rep. 2014;4:6677

[125] Tran V, Soklaski R, Liang Y, Yang L. Layer-controlled band gap and anisotropic excitons in few-layer black phosphorus. Phys. Rev. B 2014;89: 235319.

[126] Lu SB, Miao LL, Guo ZN, Qi X, Zhao CJ, Zhang H, Wen SC, Tang DY, Fan DY. Broadband nonlinear optical response in multi-layer black phosphorus: an emerging infrared and mid-infrared optical material. Opt Express. 2015;23:11183–11194.

[127] Zheng X, Chen R, Shi G, Zhang J, Xu Z, X. Cheng, T. Jiang. Characterization of nonlinear properties of black phosphorus nanoplatelets with femtosecond pulsed Z-scan measurements. Opt Lett. 2015;40:3480–3483.

[128] Sotor J, Sobon G, Macherzynski W, Paletko P, Abramski KM. Black phosphorus a new saturable absorber material for ultrashort pulse generation. arXiv:1504.04731 [cond-mat.mtrl-sci].

[129] Yu H Zheng X, Yin K, Cheng X, Jiang T. Thulium/holmium-doped fiber laser passively mode locked by black phosphorus nanoplatelets-based saturable absorber. Appl Opt. 2015;54:10290.

[130] Wang Z, Zhao R, He J, Zhang B, Ning J, Wang Y et al. Multi-layered black phosphorus as saturable absorber for pulsed Cr:ZnSe laser at 2.4 μm. Opt Express. 2016;24:1598.